DETECTING AND MEASURING TRANSVERSE AEOLIAN RIDGES (TARS) ON MARS USING DEEP LEARNING.

Alexander. M. Barrett[1], Elena. A. Favaro[1], Matthew R. Balme[1]. [1] The Open University School of Physical Sciences, Walton Hall, Milton Keynes, MK76AA, UK, alexander.barrett@open.ac.uk

Introduction: Transverse Aeolian Ridges (TARs) [1] are found across the martian surface. Terrestrial analogues show that these ridges form perpendicular to the direction of prevailing wind, and so provide a geomorphological marker for past and present wind conditions on Mars [2]. TARs are easily recognized, however digitizing them in statistically significant numbers can be extremely time consuming (for example, to extract direction data). Consequently, we developed a deep learning (DL) TAR detection system to more rapidly acquire wind direction datasets over large geographic areas. Importantly, we used a commercial, off-the-shelf (COTS) DL framework rather than a bespoke system, to see whether a shareable, scalable DL method could be achieved.

Methods: We applied the DL tools in ArcGIS Pro 3.0 to automatically segment TARs in images from the High-Resolution Imaging Science Experiment (HiRISE) camera [3]. HiRISE captures satellite images at a native resolution of 25 cm/pixel making it ideal for identifying small features such as TARs.

An existing dataset of digitized TARs was utilized as the training data for this project, using the site at Oxia Planum where we have previously studied and digitized aeolian features with DL [4]. A small section of HiRISE image ESP_037703_1980_RED was selected as the training area. This region consists of a wide valley containing several thousand TARs. Approximately 1000 TARs were selected, filtering out those which were too small to be easily recognizable, or which merged together into larger ripple fields. A size threshold of 5 m across the ridge (short axis) was chosen as the lower cut off for selected features.

Several data augmentation procedures were implemented to turn these vector shapes into a workable DL training dataset. First the HiRISE image was progressively down-sampled in 1-meter steps, creating a set of images ranging in resolution from 1 to 6 m per pixel. When the native 25 cm per pixel image was also included this provided 7 versions of the image, where the features of interest appeared at various scales relative to the size of the pixels.

The vector shapefiles segmenting the ripples were used to export a set of training frames featuring these landforms. Most of the training features are orientated east-west in the valley, with up to 45 degrees variation in places. ArcGIS DL tools are able to export rotated versions of these frames, and so a rotation factor of 315 degrees was used to ensure that there was more variety in the orientation of the training features. This allowed the network to be more transferable to other regions where TARs have different orientations.

These training frames were used to train a Mask R-CNN (Region-Based Convolutional Neural Network) model based on a Resnet 50 backbone. The model was trained for 20 epochs, although it was found to converge far faster than this, and so could have been stopped sooner.

Results: The model was found to perform well on the areas of ESP_037703_1980_RED which were not covered by the training area. It performed similarly for other images of Oxia Planum, and Jezero Crater where it could be compared to existing classification products from our past projects [4, 5].

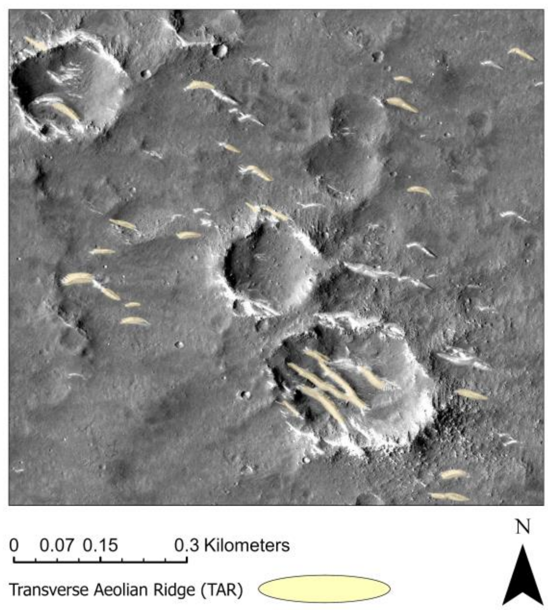

Figure 1: Classification of TARs in ESP_069731_2055__RED. Most large, regular features are detected. Some small features are below the classification threshold, while some larger features show signs of degradation, which prevent them from being classified.

Five images of the Tianwen-1 landing site [6] in Utopia Planitia were selected as a new test area. This site consists of the flat northern plains of Mars, superposed by many isolated TARs. A significantly large proportion of these were estimated to be large enough to be detected by the network. The images were then run through the network, producing a vector dataset showing the distribution of detected TARs. An example area is shown in figure 1.

Mask R-CNN in ArcGIS produces a classification product as a vector shapefile, showing the extent of the detected features. These are produced in multiple parts due to the field of view of the model and are combined into single features using the dissolve tool.

Most of the features larger than the training set's size threshold (5 m short axis) were detected. However, there were some false negatives: these typically occurred in locations where bedforms were particularly exposed, and had a rugged or windswept appearance, resulting in their structure being degraded, and their appearance not being pristine.

This is unsurprising, since few of the features in the training dataset had this "weathered" appearance. While a human can recognize that they are a more degraded form of the same feature, the deep learning system presently cannot. The training dataset could be expanded to include examples of more degraded features, in order to detect this expression of what a TAR can look like. A variety of forms where TARs interact and intersect to form rectilinear patterns could also be included, since such patterns are seen in other parts of the planet.

Some false positives were observed, though these were fewer than the false negatives. In some places, other linear features were incorrectly classified as TARs; for example, some crater rim segments. False positives were rare enough as to not be a statistically significant fraction of our measured TAR population. Therefore, they should have a negligible effect on generalized orientation estimates. The false positives are also distinct enough that a human user can filter them out with relatively little effort if, for example, a formal map is to be produced.

In terms of orientation data, the directionality of those degraded features which the DL tool failed to identify generally match those of the less degraded TARs which were detected. Consequently, the detected features provide a sufficiently representative sample of all TARs at the site, and further classification was not required to generate useful wind direction statistics. This is not expected to be true at every site, and so will require further testing when the DL is applied more widely.

Wind direction statistics: Since TARs form transverse to the prevailing wind direction [2], the orientation of their short axis can be used to infer the direction of the wind. Bounding boxes were plotted around each digitized TAR, and the orientation of the short axis was used to compute mean wind direction statistics across the site [e.g. 2] (with 180 degree ambiguity, since TARs are symmetrical) The results of this analysis are shown in figure 2.

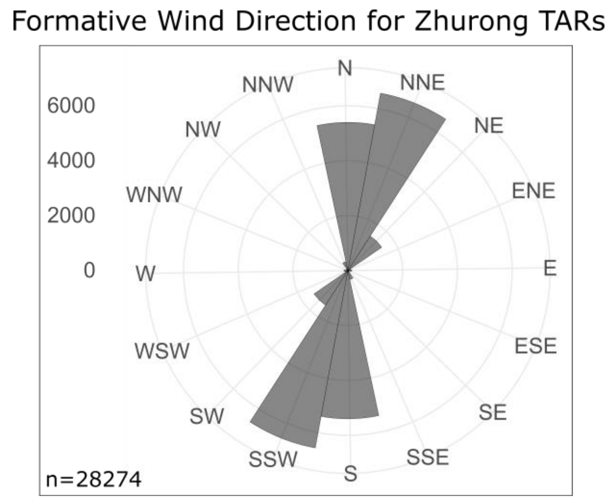

Figure 2: frequency of TAR short axis frequency for 5 HiRISE images around the Zhurong/Tianwen-1 Landing Site. Values on the concentric circles denote frequency of occurrence. Orientation shows direction from which winds are inferred to blow. (*ESP_066331_2055_RED, ESP_069876_2055_RED, ESP_069731_2055_RED, ESP_069665_2055_RED, and 069111_2055_RED.)*

The majority of features are orientated WNW-ESE (fig 1), the direction transverse to their crest (fig 2) is thus NNE-SSW.

Conclusions: In this small study, we were able to rapidly and reliably extract TAR orientations from HiRISE images using a COTS DL system. As the ArcGIS DL tools we used are widely available within many planetary science groups, this will allow trained models to be shared easily and to extend the study to regional or global scales.

Acknowledgments: We would like to thank the HiRISE instrument team for their excellent work imaging the surface of Mars. All HiRISE images used in this study are available at: https://www.uahirise.org/ and are credited to NASA/ JPL/ University of Arizona. The authors acknowledge UK funding from STFC (ST/T000228/1; AMB, MRB) and the UK Space Agency (ST/T002913/1, ST/V001965/1, ST/R001413/1; MRB, EAF)

References: [1] Balme M. et al. (2008) *Geomorphology*, *101*(4), 703–720. [2] Favaro, E. A. et al. (2021) *JGR Planets*, *126*(e2020JE006723). [3] McEwen, A. S. et al. (2007) *JGR Planets*, *112*(5), 1–40. [4] Barrett, A. M. et al. (2022) *Journal of Maps*, 1–14. [5] Wright, J. et al. (2022) *Journal of Maps*, *18*(2). [6] Liu, J. et al. (2022) *Nature Astronomy*, *6*(1), 65–71.